AGU ADVANCING EARTH AND SPACE SCIENCES

Geophysical Research Letters

RESEARCH LETTER
10.1029/2024GL110333

An Ocean Memory Perspective: Disentangling Atmospheric Control of Decadal Variability in the North Atlantic Ocean

Hemant Khatri[1], **Richard G. Williams**[1], **Tim Woollings**[2], **and Doug M. Smith**[3]

[1]Department of Earth, Ocean and Ecological Sciences, School of Environmental Sciences, University of Liverpool, Liverpool, UK, [2]Department of Physics, University of Oxford, Oxford, UK, [3]Met Office, Hadley Centre, Exeter, UK

Key Points:

- New ocean memory framework accounts for local response due to air-sea fluxes and far-field response due to ocean circulation
- The framework is employed to quantify subpolar North Atlantic Ocean thermal variability due to the North Atlantic Oscillation (NAO)
- The framework captures the sign reversal in the correlation between the NAO and ocean temperatures across seasonal to decadal timescales

Supporting Information:

Supporting Information may be found in the online version of this article.

Correspondence to:

H. Khatri,
hkhatri@liverpool.ac.uk

Citation:

Khatri, H., Williams, R. G., Woollings, T., & Smith, D. M. (2024). An ocean memory perspective: Disentangling atmospheric control of decadal variability in the North Atlantic Ocean. *Geophysical Research Letters*, *51*, e2024GL110333. https://doi.org/10.1029/2024GL110333

Received 16 MAY 2024
Accepted 27 SEP 2024

Abstract An ocean memory framework is proposed to reveal the atmosphere's influence on ocean temperatures. Anomalous atmospheric forcing alters the ocean state through two mechanisms: short-term, local effects involving air−sea heat fluxes and Ekman circulation, and long-term, far-field effects involving changes from overturning and gyre circulations. The framework employs the Green function's method to incorporate both effects, enabling the quantification of ocean memory and the contribution of atmospheric forcing to ocean thermal variability. The framework is employed to examine the North Atlantic Oscillation's (NAO) influence on the North Atlantic Ocean variability, including the Atlantic Multidecadal Variability, with its memory estimated to be 10–20 years. The NAO and variability in the North Atlantic jet speed explain up to 30% of ocean decadal variability, primarily driven by temporal changes in ocean heat transport. Therefore, decadal fluctuations in ocean temperatures cannot be accurately modeled solely as a passive response to stochastic atmospheric forcing.

Plain Language Summary The atmosphere and ocean are intricately linked, with the ever-changing atmosphere driving fluctuations in ocean temperatures. However, the atmosphere changes much faster than the ocean due to their different timescales and the ocean's ability to store excess heat for many years commonly referred to as ocean memory. As a consequence, isolating and understanding how short-term atmospheric variations influence long-term fluctuations in ocean temperatures, particularly on decadal timescales, can be difficult. To address this challenge, we introduce an ocean memory framework that allows us to analyze and quantify the atmosphere's contribution to ocean variability. We apply this framework to study how the North Atlantic Oscillation, a major atmospheric pattern in the northern hemisphere, influences decadal fluctuations in the subpolar North Atlantic Ocean temperatures. We estimate the ocean memory timescale in the subpolar North Atlantic to be about 10–20 years, which is how long temperature anomalies persist, while being redistributed, in the ocean before dissipating.

1. Introduction

There is a long-standing debate about the relative contributions of atmospheric forcing and ocean circulation in controlling decadal fluctuations in North Atlantic sea surface temperatures (SSTs), a phenomenon known as the Atlantic Multidecadal Variability (AMV) (Delworth & Mann, 2000; Knight et al., 2006; Monerie et al., 2019; Zhang & Delworth, 2006). A frequent argument asserts that the AMV is simply a "local thermal response" of a passive ocean to stochastic atmospheric forcing (Cane et al., 2017; Clement et al., 2015), which produces a red-noise response in SST spectrum, with most of the variance concentrated in interannual-decadal timescales (Frankignoul & Hasselmann, 1977). An alternative view emphasizes the importance of a dynamically-active ocean, with low-frequency changes in ocean circulation, such as the Atlantic meridional overturning circulation, influencing North Atlantic SSTs by transporting anomalous heat across the tropics (Delworth et al., 2017; O'Reilly et al., 2016; Robson et al., 2016; Zhang, 2017). However, the relative importance of atmospheric forcing and ocean processes in driving the AMV remains unclear.

To reconcile these differing perspectives, we propose an ocean memory framework that quantifies atmospheric-driven ocean state variations, which we separate in terms of local, fast and far-field, slow effects. Oceans are assumed to have a multi-year memory due to their high thermal inertia and long spin-up duration for ocean circulation (Hansen & Bezdek, 1996; Namias & Born, 1970). Heuristic estimates based on the timescales of oceanic phenomena such as El Niño-Southern Oscillation (ENSO) and meridional overturning circulation suggest that ocean memory, represented by the persistence of SST anomalies, could range from a few years to several decades (Deser et al., 2010; Jackson et al., 2022). However, a precise definition of ocean memory remains elusive,

making it challenging to quantify how relatively short-term atmospheric forcing influences decadal ocean variability. Previous works have estimated ocean memory by calculating lagged auto-correlations of SST anomalies (Shi et al., 2022). However, the auto-correlation approach only measures the local persistence of SST anomalies and cannot account for far-field effects, such as the delayed redistribution and advection of temperature anomalies (Khatri et al., 2022). In the proposed framework, we precisely quantify ocean memory as the timescale of the decay of ocean temperature anomalies triggered by a single external atmospheric perturbation, including both local and far-field effects.

We present a case study of the subpolar North Atlantic Ocean, which exhibits pronounced variability on interannual-multidecadal timescales involving changes in the ocean heat content and meridional overturning circulation (Fraser & Cunningham, 2021; Jackson et al., 2022; Lozier et al., 2008; R. G. Williams et al., 2014). The North Atlantic Oscillation (NAO), which is the dominant mode of atmospheric variability in the Atlantic sector (Hurrell, 1995; Hurrell & Deser, 2010), plays a key role in driving decadal variability in the North Atlantic Ocean (Eden & Jung, 2001; Marshall, Johnson, & Goodman, 2001; McCarthy et al., 2015). The impact of seasonal NAO perturbations can last for many years in the subpolar North Atlantic Ocean through a combination of anomalous heat fluxes and Ekman circulation, referred to as a local, fast effect, and subsequent delayed changes in the overturning and gyre heat transport, referred to as a far-field, slow effect (Khatri et al., 2022; Kim et al., 2024; Roussenov et al., 2022). Thus, the subpolar ocean is well suited for analyzing the relative contributions of atmospheric forcing and ocean processes in driving ocean temperature variations.

We analyze the role of the NAO in driving decadal thermal variability in the subpolar North Atlantic Ocean. Utilizing NAO-based composite analyses (following Khatri et al., 2022) and linear response theory (Hasselmann et al., 1993; Leith, 1975), we develop a simplified NAO-based heat budget model for the upper ocean. This model is used to reconstruct ocean temperature timeseries from NAO history and quantify the contributions of NAO-induced local and far-field effects to thermal variability in the subpolar North Atlantic Ocean. We find that the NAO explains up to 30% of the decadal variability in upper ocean temperatures in the subpolar North Atlantic.

2. Methodology

2.1. Description of Observations and Models

Our analysis of how the atmosphere influences ocean variability is applied to both observations and coupled climate model outputs. Ocean temperature (HadISST and EN4 data sets, Rayner et al., 2003; Good et al., 2013) and sea level pressure (HadSLP2 data set, Allan & Ansell, 2006) observations are analyzed. Additionally, outputs from four different Coupled Model Intercomparison Project Phase 6 (CMIP6) models—HadGEM3-GC31-MM (K. Williams et al., 2018), GFDL-CM4 (Held et al., 2019), IPSL-CM6A-LR (Boucher et al., 2020) and NCAR-CESM2 (Danabasoglu et al., 2020) are used to make comparison against observations. The selected models differ in terms of horizontal grid resolution, numerical and parameterization schemes allowing to test our methodology on a relatively diverse set of climate models. More details on these observational data sets and climate models are provided in Table S1 in the Supporting Information S1.

2.2. NAO-Based Composite Analysis

Following the methodology of Khatri et al. (2022), composite analyses are used to examine the impact of a single NAO+ event on the subpolar ocean temperatures in observational data and historical climate simulations (Figure 1). Domain-averaged upper 200 m temperature anomalies, referred to as θ' here, and domain-averaged SST anomalies in the subpolar region (45°N–70°N, 80°W–0°) are examined. For observation-based composites, NAO composites were created using HadSLP2 data and the same time information was then used to create composites of θ' and SST$'$ from EN4 and HadISST data sets, respectively.

A NAO+ event initially leads to anomalous cooling in the upper subpolar ocean (area enclosed within the rectangle, Figure 1e). In subsequent years, opposing-signed positive temperature anomalies form due to anomalous heat convergence into the subpolar ocean (see Khatri et al., 2022). These immediate cooling and subsequent warming trends are observed uniformly across the entire subpolar region (Figures 1e–1j), which motivated our choice to analyze the decadal variability in this region.

The subpolar North Atlantic Ocean exhibits multi-year memory, as evidenced by temperature anomalies induced by a seasonal NAO event dissipating over 8–10 years due to anomalous ocean heat transport (see Figure 3 in

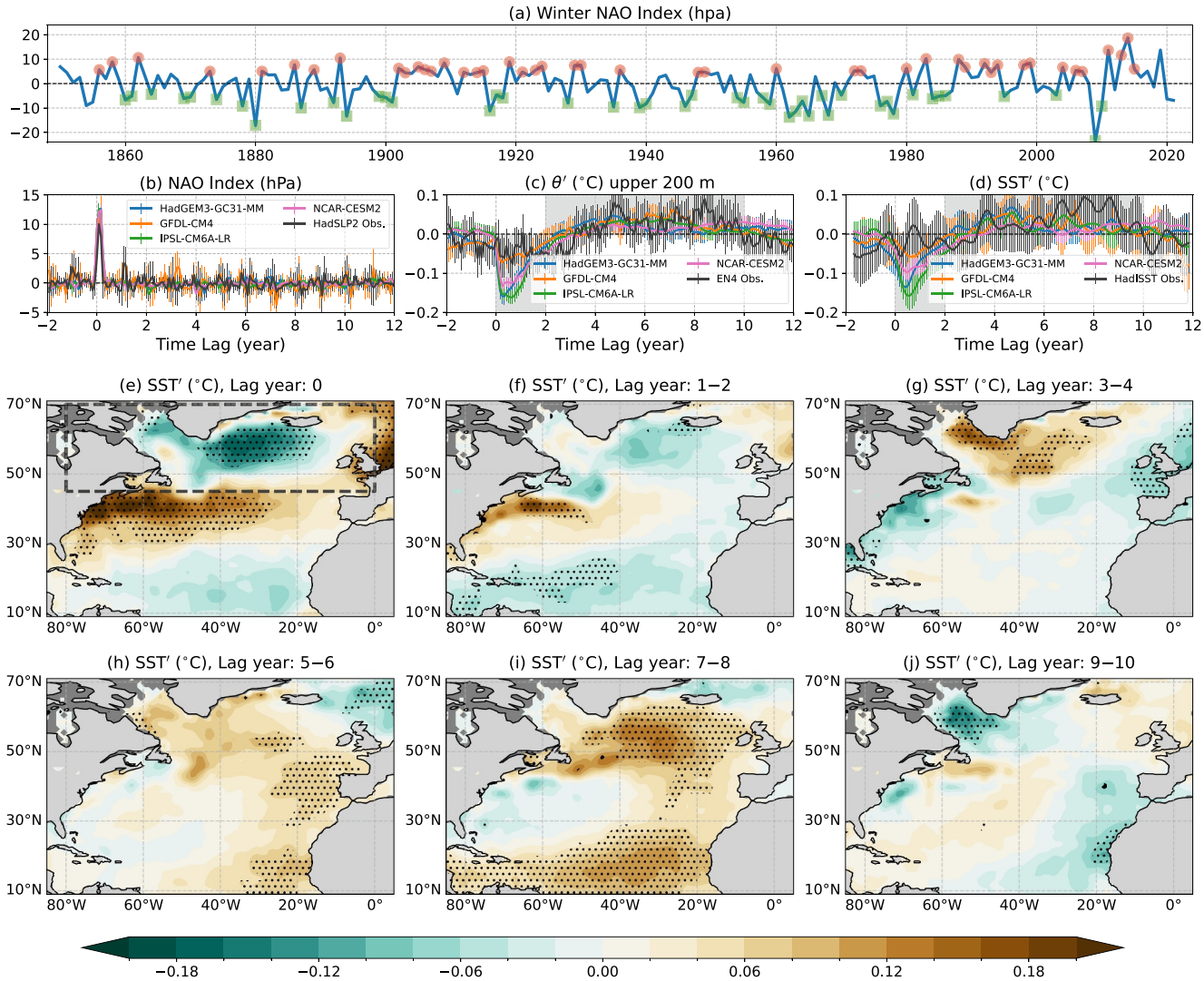

Figure 1. Subpolar North Atlantic Ocean response to a single NAO+ event in observations and CMIP6 historical simulations: (a) Winter (Dec-Jan-Feb mean) NAO index from HadSLP2 data set; (b) NAO composites (created by aligning NAO extremes outside one standard deviation, see circle and square markers in panel (a)); (c) Composites of monthly domain-averaged temperature anomalies in the upper 200 m in the subpolar ocean (45°N–70°N, 80°W–0°, area enclosed within the rectangle in panel (e)); (d) Composites of monthly domain-averaged subpolar SST anomalies (smoothed with 6-month running window for clear visualization); (e–j) Annual-mean composites of SST anomalies from HadISST data at different lag years after the onset of a single NAO+ event. Errorbars in panels (b–d) and stipplings in panels (e–j) denote that anomalies are significant at 95% confidence level. Note that composites are created by subtracting NAO− members from NAO+ members. NAO indices were computed as the difference between the mean sea-level pressure anomalies between Azores (36°N–40°N, 28°W–20°W) and Iceland (63°N–70°N, 25°W–16°W) regions. Linear trends, climatology, and temporal variations longer than 20 years were removed to filter out multi-decadal trends before creating composites.

Khatri et al., 2022). These findings support previous studies (Delworth et al., 2017; Josey & Sinha, 2022; R. G. Williams et al., 2014; Zhang, 2017) which argued that ocean circulation, along with air−sea heat fluxes, plays a key role in regulating decadal variability in ocean temperatures. Indeed, the local effect associated with a NAO event can partially explain variations in the North Atlantic Ocean circulation (Marshall, Johnson, & Goodman, 2001; McCarthy et al., 2015). However, the ocean's local response to atmospheric forcing associated with a NAO event cannot explain the delayed generation of opposing-signed subpolar temperature anomalies (Figure 1) and their subsequent damping over decadal timescales (see Gu et al., 2024). We investigate the relative contributions of NAO-induced local and far-field effects in driving decadal thermal variability in the subpolar North Atlantic Ocean.

The SST anomaly pattern at a lag of 5−8 years after the onset of a NAO event (Figures 1h and 1i) resembles the horseshoe AMV pattern (Zhang et al., 2019). Many studies argue that the NAO is the primary driver of the AMV

(Clement et al., 2015; McCarthy et al., 2015). Therefore, insights from the present NAO-based analysis of the subpolar ocean may clarify the NAO's role in governing the AMV, given the strong correlation between subpolar SST anomalies and AMV (a correlation coefficient exceeding 0.9, computed using annual-mean SST anomalies, was shown in O'Reilly et al., 2016). Our aim is to quantify NAO-associated temperature variability in the North Atlantic Ocean and reconcile the different views of how ocean variability is controlled (Clement et al., 2015; Zhang, 2017).

3. Ocean Memory Framework

We define ocean memory as the measure of the timescale of decay of ocean temperature anomalies created directly or indirectly by atmospheric forcing associated with a NAO event. In this definition, the measured ocean memory accounts for both anomalous air−sea heat fluxes and changes in the ocean heat transport due to the NAO. In the ocean memory framework, we derive a simplified heat budget equation, which incorporates both local and far-field effects, to quantify NAO-associated thermal variability in the subpolar North Atlantic Ocean.

3.1. NAO-Based Heat Budget Model

The heat budget for the upper ocean can be written as

$$\frac{\partial \theta'}{\partial t} = \frac{1}{\rho_o C_p \Delta V}\left(\mathcal{H}' + \nabla \cdot \mathcal{T}'\right), \tag{1}$$

where θ' represents the domain-mean temperature anomaly (upper 200 m in the subpolar ocean in the present study, 45°N−70°N, 80°W−0°W), ΔV is the domain volume, $\rho_o C_p = 4.09 \times 10^6$ J kg^{-1} m^{-3} °C^{-1}. $\mathcal{H}'$ is the domain-integrated atmosphere-to-ocean heat flux anomaly and $\nabla \cdot \mathcal{T}'$ represents the domain-integrated anomalous heat convergence associated with both the horizontal and vertical components of advective and diffusive heat transport.

Khatri et al. (2022) proposed that subpolar ocean response to the NAO can be understood in terms of a fast response, related to anomalous heat fluxes and Ekman flow, and slow response, involving changes in the geostrophic overturning and gyre circulations and the associated heat convergence (see Figure 2a). Thus, we rewrite Equation 1 as the sum of the fast and slow components

$$\frac{\partial \theta'}{\partial t} = \frac{1}{\rho_o C_p \Delta V}\left(\underbrace{\mathcal{H}' + \nabla \cdot \mathcal{T}'_{\text{ekman}}}_{\text{fast comp.}} + \underbrace{\nabla \cdot \mathcal{T}'_{\text{non-ekman}}}_{\text{slow comp.}}\right), \tag{2}$$

$$\frac{\partial \theta'}{\partial t} = \mathcal{F}_{\text{fast}} + \mathcal{F}_{\text{slow}}. \tag{3}$$

The fast and slow ocean responses are viewed as equivalent to local and far-field effects, respectively. We further assume that the fast component is proportional to the NAO index, $\mathcal{F}_{\text{fast}} = \alpha$ NAO. Here, α is set to a negative constant to ensure generation of negative subpolar temperature anomalies from a NAO+ event or positive temperature anomalies from a NAO− event (Visbeck et al., 1998). Finally, the generalized form of the NAO-based heat budget can be written as,

$$\frac{\partial \theta'}{\partial t} = \alpha\ \text{NAO} + \mathcal{F}_{\text{slow}} = \alpha\ \text{NAO} + \frac{1}{\rho_o C_p \Delta V}\nabla \cdot \mathcal{T}'_{\text{non-ekman}}. \tag{4}$$

3.2. Green's Function Approach

To solve for $\mathcal{F}_{\text{slow}}$ and θ', we use linear response theory and represent θ' as the convolution of a linear response function, $\mathcal{G}$ (or Green's function) and the NAO (Frankignoul & Hasselmann, 1977; Hasselmann et al., 1993; Leith, 1975). For $\mathcal{G}$, we choose a smooth analytical function (see dashed black curve in Figure 2a, resembles a damped harmonic process) that represents the evolution of θ' over the subpolar North Atlantic Ocean after the onset of a NAO event,

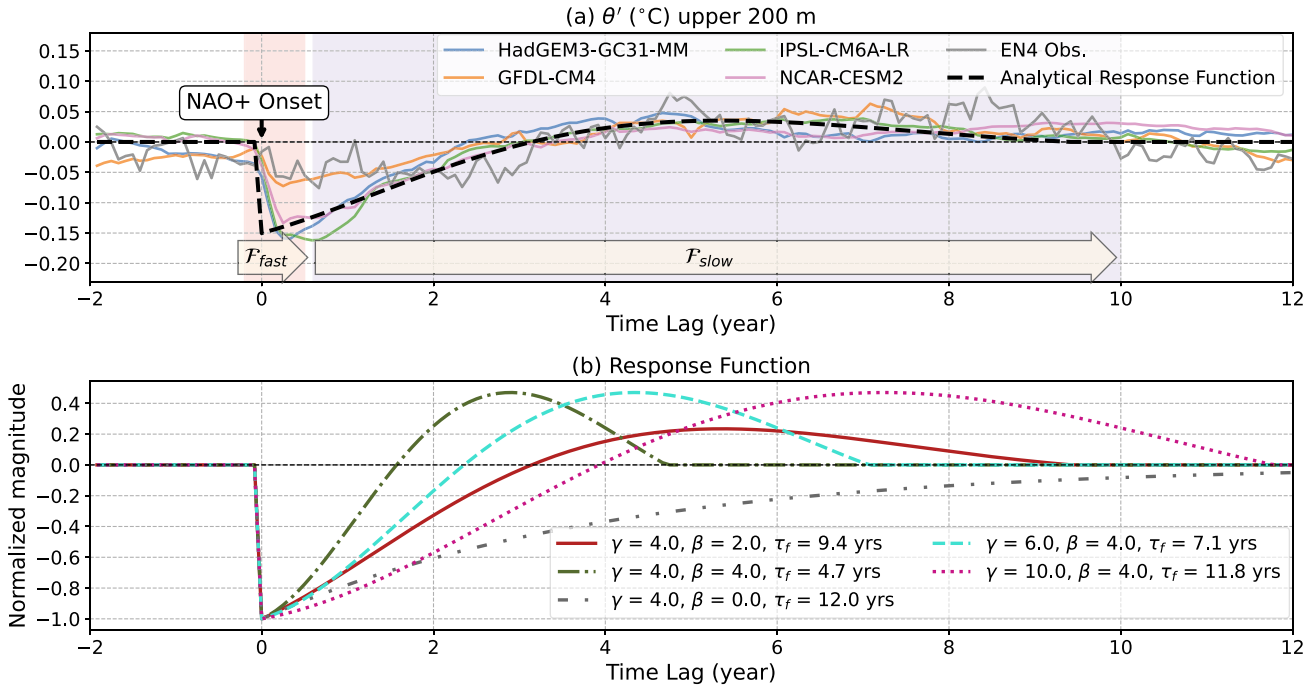

Figure 2. (a) Composites of monthly domain-averaged subpolar temperature anomalies (same as in Figure 1c). The dashed black curve represents an analytical response function to capture the temporal evolution of temperature anomalies due to a single NAO+ event; (b) Response functions for different choices of γ and β parameters and the associated ocean memory, $\tau_f = 3\pi\gamma/2\beta$. The negative of the response function is plotted for easier comparison against θ' composite-means in panel (a).

$$\mathcal{G}(t) = e^{-t/\gamma}\cos\left(\frac{\beta}{\gamma}t\right) \quad \text{if} \quad 0 \le t \le \frac{3\pi}{2}\frac{\gamma}{\beta}$$
$$= 0 \quad \text{otherwise} \tag{5}$$

We can then reconstruct θ' as the convolution of the NAO time-series and $\mathcal{G}$,

$$\theta'(t) = \alpha \int_0^t \mathrm{NAO}(t - t_1)\,\mathcal{G}(t_1)\,\mathrm{d}t_1. \tag{6}$$

The Green's function approach has been employed to investigate how atmospheric variability or large-scale atmospheric modes influence SSTs in the Southern Ocean (Kostov et al., 2017) and the Arctic freshwater content (Cornish et al., 2020; Johnson et al., 2018). However, unlike in previous studies, we use a smooth analytical form for $\mathcal{G}$ to have a well defined timescale of ocean response, denoted by $\tau_f = 3\pi\gamma/2\beta$ and is equal to three-fourths of the wavelength of the cosine function in Equation 5. Here, γ and β parameters control the shape of the response function and mimic the effect of NAO-induced anomalous air−sea heat fluxes and ocean heat transport on θ' evolution. While the chosen response function is effective for this study, alternative analytical functions could be equally suitable. Alternative choices might be better suited for specific situations, such as subtropical gyres or zonal current systems.

Another advantage of using an analytical response function is that there exists a governing equation for the temperature evolution revealing a functional form for $\mathcal{F}_{\mathrm{slow}}$ (substitute Equation 6 into Equation 4, full derivation is in the Supporting Information S1),

$$\frac{\partial\theta'}{\partial t} = \alpha\,\mathrm{NAO} \underbrace{-\frac{\theta'}{\gamma} - \frac{\alpha\beta}{\gamma}\int_0^t \mathrm{NAO}(t - t_1)e^{-t_1/\gamma}\sin\left(\frac{\beta}{\gamma}t_1\right)\mathrm{d}t_1}_{\mathcal{F}_{\mathrm{slow}}}. \tag{7}$$

Here, γ simply acts as a damping timescale, while β governs the reversal in the sign of temperature anomalies (Figure 2b). Together, these parameters determine the relative magnitudes of the initial and delayed opposing-signed temperature anomalies allowing us to properly incorporate NAO-induced ocean contributions in driving upper ocean temperature variability via anomalous heat convergence and estimate true ocean memory. Note that integrating Equation 7 leads to an additional term, $\theta'(0)e^{-t/\gamma}$, in Equation 6. This additional term represents a boundary condition at $t = 0$, which damps out in a few years and is not important for the analysis presented here. Moreover, the Green's function approach assumes a linear relationship between the atmospheric forcing and ocean response, therefore not considering potential feedback of the ocean on the atmosphere.

The functional form (Equation 7) represents a wide range of possible solutions depending on γ and β magnitudes, each with a different skill. One limiting case is explored below.

3.2.1. Limit of $\beta = 0$

By setting $\beta = 0$, we obtain the classical Hasselmann model (Frankignoul & Hasselmann, 1977; Hasselmann, 1976). The Hasselmann model assumes that stochastic atmospheric forcing drives variability in upper ocean temperatures, with atmospheric-induced ocean temperature anomalies eventually damped over a fixed timescale ($\mathcal{F}_{\text{slow}} = -\theta'/\gamma$, gray dash-dot-dot curve in Figure 2b). The damping timescale γ is empirically set to 4 years to match the observed temperature variability in the North Atlantic Ocean (Clement et al., 2015; O'Reilly et al., 2016); however, a theoretical justification for the specific value of γ remains elusive. Recently, Shi et al. (2022) estimated damping timescales of 2–3 years using lagged correlations of SST anomalies in the subpolar ocean. Since the atmosphere damps upper ocean temperatures over timescales of few months (Gu et al., 2024), these relatively long damping timescales are likely set by ocean processes (Liu et al., 2023; Zhang, 2017). Our composite analysis provide a justification for using damping timescales within a range of 2–4 years in stochastic models (Figure 2a, also see Khatri et al., 2022).

3.3. Timescales of Ocean Memory

NAO-based reconstructions of θ' from Equation 6 are used to estimate subpolar ocean memory. γ and β parameters are optimized to maximize the correlation between the reconstructed and actual θ'. The square of correlation coefficient provides a measure of ocean temperature variance captured by the NAO and an estimate of ocean memory is provided by the resulting value of $\tau_f = 3\pi\gamma/2\beta$. In practice, we use the following approach to avoid unrealistically large estimates of τ_f,

$$\tau_f = \text{Min}\left(\frac{3\pi}{2}\frac{\tau}{\beta},\ 3\gamma\right). \tag{8}$$

For $\beta = 0$ or very small values of β, we use $\tau_f = 3\gamma$, which corresponds to decay of anomalies by 95%. Also, for reconstructing θ' at time t, we only consider the NAO time-series for the past $\tau_f = 3\pi\gamma/2\beta$ years by setting $\mathcal{G} = 0$ at $t > \tau_f$. This time window is equal to three-fourths of the wavelength of the cosine function in Equation 5 and is expected to be on the order of 10 years based on composite analyses (Figure 1).

Many studies have developed simplified models to contrast between atmospheric and oceanic contributions in driving ocean temperature variability (Liu et al., 2023; O'Reilly et al., 2016; Saravanan & McWilliams, 1998). However, these models do not distinguish between ocean contributions due to internal ocean variability and atmospheric-induced changes in ocean circulation, with timescales of ocean variability often chosen empirically. On the other hand, our NAO-based heat budget (Equation 6) only considers variations in ocean heat transport induced by the NAO (i.e., atmospheric forcing), with timescales associated with local, fast and far-field, slow effects derived from composite analyses (Figure 2). These NAO-induced changes in ocean heat transport can be attributed to two mechanisms: (a) changes in the strength of overturning and gyre circulations (R. G. Williams et al., 2015), and (b) the redistribution of subpolar-subtropical temperature anomalies by the background circulation and the resulting modifications in zonal temperature gradients (Khatri et al., 2022). Our approach allows us to consider time-varying ocean circulation and heat transport for studying its effect on ocean thermal variability.

4. NAO-Based Reconstruction of Ocean Temperatures

Subpolar ocean temperature anomaly, θ', time-series is reconstructed for a range of γ and β values using Equation 6. These reconstructions are based on the NAO time-series from HadSLP2 data and climate model outputs. The correlations between the reconstructed and actual θ' monthly time-series are computed to identify γ and β values that maximize this correlation (Figure 3). These optimal values are then used to reconstruct the θ' time-series and the associated τ_f magnitude provides an estimate for ocean memory. The maximum correlation lies along isolines of τ_f, suggesting that there is narrow range of optimum timescales for ocean memory, essentially the duration over which temperature anomalies persist in the ocean, while being redistributed by the ocean circulation, following a seasonal NAO perturbation. In addition, we set the value of α such that the standard deviations of the reconstructed and actual θ' are equal. However, the correlations are not sensitive to α.

4.1. Ocean Memory for the Subpolar North Atlantic

Analyses of observational data (HadSLP2 and EN4) indicate ocean memory of approximately 18 years while ocean memory estimates from climate models are in the range of 8–12 years (Figure 3 and Table S2 in the Supporting Information S1). This decade-long ocean memory is likely set by overturning and gyre circulations and the associated heat transport in the ocean (Khatri et al., 2022; Zhang et al., 2019), as the damping effect of seasonal-interannual atmospheric perturbations on ocean surface anomalies is insufficient to explain the long-term persistence of temperature anomalies (Gu et al., 2024). Our ocean memory estimates are also consistent with O'Reilly and Zanna (2018), who found a peak response in North Atlantic SSTs due to atmospheric forcing at a timescale of 20 years in observations, compared to only 10 years in CMIP5 models.

Our estimated ocean memory significantly exceeds previous values based on lagged auto-correlation of SST anomalies (Shi et al., 2022), suggesting that relying solely on lagged auto-correlations underestimates ocean memory. One caveat to note is that we only considered θ' reconstructions that are correlated with the actual θ' with a correlation coefficient greater than 0.4 (see Figure 3 caption) and computed ocean memory using the associated γ and β parameter values. These ocean memory estimates are, however, relatively insensitive to the chosen correlation coefficient threshold, with observations consistently indicating a higher ocean memory than climate models (Table S3 in the Supporting Information S1).

4.2. Skill of NAO-Based Reconstructions

The maximum correlations between the reconstructed and actual θ' time-series are in range 0.33–0.54 (on timescales longer than 5 years) for both observations and CMIP6 models (see dashed green and solid back curves in Figures 3a1–3e1). Thus, 15%–30% variance of the area-averaged temperatures in the upper subpolar North Atlantic Ocean can be explained in terms of the NAO, supporting the notion that atmospheric forcing plays a significant role in governing ocean thermal variability. Since the NAO captures 30%–40% of the atmospheric variability in the North Atlantic (Hurrell & Deser, 2010), there is an upper bound on the ocean variability explained by the NAO. To estimate the overall atmospheric-driven ocean variability, one would need to account for higher modes of atmospheric variability, such including the East Atlantic and Scandinavian blocking patterns (Barrier et al., 2014), by expressing Equation 6 as a linear combination of convolutions of different Green's functions and atmospheric modes. However, this would require determining optimal values for many more parameters, which could be difficult and computationally expensive.

It is crucial to account for sign-reversal in temperature anomalies after the onset of a NAO event (maximum correlation occurs at $\beta > 0$, Figure 3), indicating far-field effects associated with ocean processes play a substantial role in ocean temperature variability. Excluding the far-field effect by not considering the sign-reversal in temperature anomalies (setting $\beta = 0$ and $\gamma =$ 1–6 years, which cover damping timescale estimates from Clement et al., 2015; O'Reilly et al., 2016; Shi et al., 2022) significantly reduces the correlations (in range 5%−10%) and the NAO captures 5%−10% of the decadal variability in ocean temperatures (see dashed gray and solid back curves in Figure 3a1–3e1). Also, note that the maximum correlations for higher-resolution climate models (HadGEM3 and GFDL-CM4, with correlations in the range 0.53–0.54) are significantly higher than those for lower-resolution models (IPSL and NCAR, with correlations in the range 0.33–0.39). This suggests that low-resolution models underestimate the NAO-driven low-frequency variability in subpolar North Atlantic Ocean temperatures and may not accurately represent the ocean's response to the NAO (also see Patrizio et al., 2023).

10.1029/2024GL110333

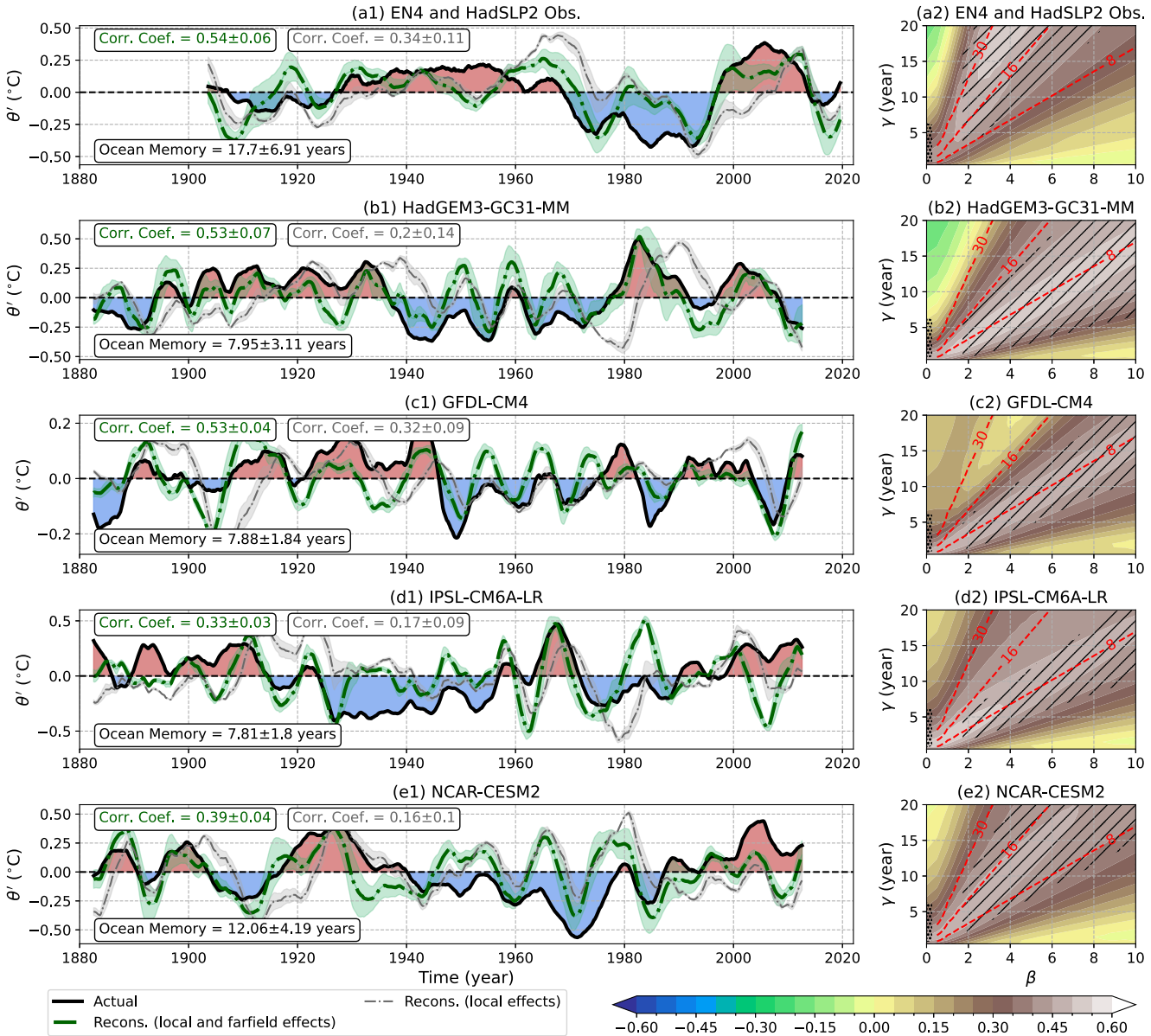

Figure 3. (a1–e1) Actual and reconstructed temperature anomalies in the upper 200 m subpolar North Atlantic Ocean for observations and r1 ensemble historical climate simulations (linear trends and timescales shorter than 5 years were removed, reconstructed θ' were normalized to match the standard deviation of the actual θ' time-series). (a2–e2) Correlations between the actual and reconstructed θ' (monthly detrended time-series of θ' were used for calculating correlations). The correlation maps are averaged for all available historical ensemble simulations for each model (see details in the Supporting Information S1). In panels (a2–e2), red dashed curves correspond to constant ocean memory timescales. Black hatching represents γ and β parameter values (chosen based on correlation ≥ 0.4 with p-value ≤ 0.01 and $\gamma \geq 1.0$ years to avoid excess dissipation of temperature anomalies) considered for reconstructing θ' and estimating ocean memory (see green curves in panels (a1–e1), both local and far-field effects, shading presents ± standard deviation). Black stippling (at $\beta = 0$) represents γ values considered for reconstructing θ' (see gray curves in panels (a1–e1), local effects only). Note that correlations and variances in panels (a1–e1) are for low-pass filtered time-series (timescales longer than 5 years retained).

The atmosphere is viewed as playing a prominent role in driving SST variability on seasonal-interannual timescales, whereas the ocean plays a prominent role on decadal timescales (Bjerknes, 1964; Khurshut, 1994). This shift in dominance is revealed by a change in the sign of the correlation between the NAO and SST anomalies, with negative correlations for interannual variability and positive correlations for decadal variability (Delworth et al., 2017; Gulev et al., 2013; O'Reilly et al., 2016). Our NAO-based heat budget model effectively captures this sign reversal in the correlation between the NAO and subpolar ocean temperature anomalies (Figure 4 and Figure S1 in the Supporting Information S1). Notably, low-pass filtering (retaining timescales greater than 10 years) reveals a positive correlation between the NAO and θ' at time lag of 5–15 years, with the NAO leading θ' (Figure 4,

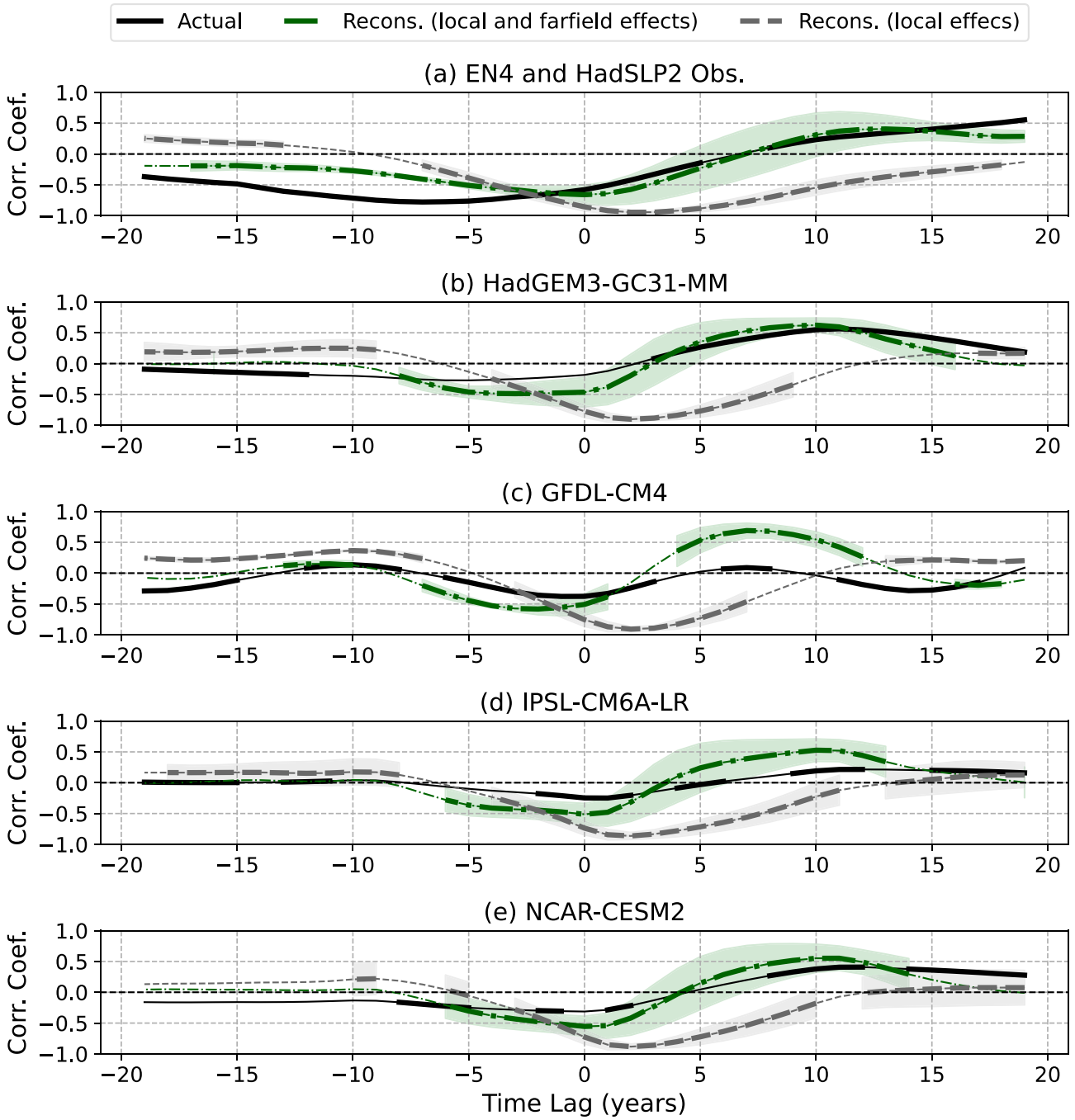

Figure 4. Lead-lag correlations between the NAO and θ' (a) observations (b–e) historical climate simulations. Correlations are for low-pass time-series (timescales greater than 10 years retained). NAO leads temperature anomalies for positive lag years. All available historical ensembles are considered with black curves representing the ensemble-mean correlations (thick lines are significant at 95% confidence level, p-value ≤ 0.05). Shading in correlations for the reconstructed time-series represents ± standard deviation, computed as described in Figure 3.

also see Figure 3 in Delworth et al., 2017). The correlations from the reconstructed temperature anomalies are consistent with correlations from the actual ocean temperature anomalies in both observations and models (compare black and green curves in Figure 4). However, neglecting the sign-reversal in temperature anomalies following a NAO event leads to exclusively negative NAO–θ' correlations, consistent with results from slab ocean models (Figure 3 in Delworth et al., 2017). Note that strong negative correlations (at a lag of –5 to –15 years) in the

observational data set suggest that there might be significant ocean forcing on the atmosphere, particularly on the NAO. The absence of significant correlations at negative lag years in climate models implies that the influence of similar ocean forcing on the atmosphere is weak within these models. However, correlation analysis alone is insufficient to confirm this hypothesis. Moreover, the ocean memory approach does not consider potential ocean-to-atmosphere feedback.

Our findings demonstrate that far-field effects, linked to delayed changes in ocean circulation and heat transport, significantly influence decadal ocean temperature variations (also advocated by Delworth et al., 2017; Josey & Sinha, 2022; Zhang, 2017). Models with a passive ocean driven by stochastic atmospheric forcing (Clement et al., 2015) underestimate NAO-associated ocean thermal variability by 10%–20%. These results apply to both historical and pre-industrial control climate simulations across interannual to multi-decadal timescales. Incorporating the far-field effect in the NAO-based heat budget Equation 6 consistently captures more ocean temperature variance (Figures S3–S4 in the Supporting Information S1, note that using SSTs instead of upper 200 m temperature anomalies yields similar findings).

4.3. Application of the Green's Function Approach to Explain the Atlantic Multidecadal Variability

The NAO-based heat budget analysis can also be applied to investigate the relationship between the NAO and AMV. This is because subpolar temperature anomalies are strongly correlated with the AMV index (O'Reilly et al., 2016) and lagged SST anomalies after the NAO onset resemble the AMV spatial pattern (Figure 1). Similar to the subpolar region, correlations between the NAO and AMV index (SST anomalies averaged over the North Atlantic Ocean, 0°–70°N, 80°W–0°) show a sign reversal in both the actual and NAO-based reconstructed temperature anomalies (Figure S2 in the Supporting Information S1). This suggests that a significant portion of the AMV can be explained in terms of the NAO by appropriately accounting for local and far-field effects.

4.4. Role of the North Atlantic Jet Stream

We next explore how the atmospheric jet stream's strength and latitudinal position, governing the NAO phase (Woollings et al., 2010), influence temperature variations in the subpolar ocean. North Atlantic jet indices, defined as anomalies in the zonally averaged 850–hPa zonal wind (between 0–60°W and 15°N–75°N) and their associated latitude, are used within Equation 6 to reconstruct θ'. The subpolar ocean thermal variability can be explained by considering atmospheric jet strength variations. The reconstructed θ' using the jet speed index exhibit correlations of 0.39–0.49 with the actual θ' (see Supporting Information S1). The estimated ocean memory from jet speed indices falls within a range of 7–17 years, consistent with the memory estimates presented in Figure 3. In contrast, jet stream position variability appears to have minimal influence on ocean temperatures. Reconstructions of θ' using jet latitude anomalies show low correlations with the actual θ'. These results raise the possibility that the North Atlantic Ocean has a substantial influence on decadal variability in the jet stream's latitudinal position and provide evidence of a coupling between winter jet speed and the North Atlantic Ocean variability on decadal timescales (Woollings et al., 2015).

5. Discussion and Conclusions

The atmosphere plays a key role in driving interannual to multi-decadal fluctuations in North Atlantic Ocean temperatures because the impact of relatively short-timescale atmospheric forcing on the ocean can last for many years (Khatri et al., 2022; Robson et al., 2012). However, the timescales of ocean variability are obscured due to continuous atmosphere-ocean interactions and the relative contributions of the atmospheric forcing and ocean circulation in driving decadal fluctuations in ocean temperatures are not fully understood (Clement et al., 2015; Delworth et al., 2017).

We propose a new ocean memory framework to quantify the proportion of ocean variability driven by the atmosphere. In particular, we examine the temperature variability in the upper subpolar North Atlantic Ocean due to the North Atlantic Oscillation (NAO), which captures 30%–40% of the atmospheric variability in Atlantic sector (Hurrell & Deser, 2010). The NAO alters the ocean temperatures via anomalous heat fluxes and Ekman transport, referred to as local effect here, and via delayed changes in overturning and gyre circulations and the associated heat transport, referred to as far-field effect here, on seasonal-decadal timescales (Eden & Willebrand, 2001; Khatri et al., 2022; Marshall, Kushnir, et al., 2001). The ocean memory approach accounts for both local and far-field effects to quantify their contribution to the variability observed in ocean temperatures and estimate ocean

memory. A simplified NAO-based heat budget model employing Green function's approach (Frankignoul & Hasselmann, 1977; Hasselmann, 1976) is used to reconstruct ocean temperature anomalies from the NAO history obtained from observational data sets and climate models. It is shown that the NAO explains up to 30% of decadal thermal variability in the subpolar North Atlantic Ocean in both observations and climate models. This influence is primarily driven by variations in the speed of the North Atlantic jet stream.

Our findings indicate that seasonal to interannual variability in ocean temperatures is primarily driven by air−sea heat fluxes and Ekman transport associated with the NAO (Figure 1). On decadal and longer timescales, however, ocean processes such as the meridional overturning and gyre circulations exert a significant influence on ocean temperatures (as previously argued by Zhang, 2017; Zhang et al., 2019). The redistribution of subpolar–subtropical ocean temperature anomalies, triggered by the NAO, alters the ocean heat transport, leading to anomalous heat convergence and formation of opposing-signed temperature anomalies in the subpolar North Atlantic Ocean (see Khatri et al., 2022). Consequently, the correlation between the NAO and subpolar temperature anomalies exhibits a sign reversal, with negative correlations for interannual variability and positive correlations for decadal variability (Figure 4). A similar sign reversal in correlations between the NAO and Atlantic Multidecadal Variability (AMV) index is also observed. Hence, stochastic climate models that assume a passive ocean responding to atmospheric forcing (Cane et al., 2017; Clement et al., 2015) underestimate the atmospheric-driven thermal variability in the ocean, especially on decadal timescales.

Although we only consider atmospheric-driven local and far-field influences on ocean temperatures, our ocean memory approach effectively captures the sign-reversal in NAO-ocean temperature correlation across interannual to decadal timescales (Delworth et al., 2017; Gulev et al., 2013). Therefore, a significant portion of decadal variations in ocean temperatures can be explained by local and far-field ocean responses to atmospheric variability and consideration of ocean circulation variability independent of atmospheric forcing is not necessary (also see Gozdz et al., 2024). This finding helps reconcile differing perspectives on the relative importance of atmospheric forcing and ocean circulation in driving the AMV (Clement et al., 2015; Zhang, 2017). Our methodology might also be useful for Pacific and Southern Oceans, which show similar decadal variability (Gu et al., 2024) and could benefit from separating the local and far-field atmospheric influences on the ocean.

Moreover, our ocean memory framework allows us to accurately measure the decay timescales of ocean temperature anomalies (termed ocean memory here) resulting from a NAO event. Ocean memory in the subpolar North Atlantic is estimated to be approximately 18 years based on observations, while climate models suggest a range of 8–12 years (Figure 3). In the North Atlantic, ocean memory is possibly set by the timescales of variability in the ocean heat transport (Gu et al., 2024; Khatri et al., 2022; Zhang et al., 2019). However, ocean memory might differ in other oceanic regions due to variations in the background ocean circulation, involving overturning and gyre circulations, and basin size.

Furthermore, the significant discrepancy between ocean memory in observations and climate models suggests that climate models may be too dissipative in terms of ocean memory. This means climate models lose excess heat from the ocean faster than the real world, potentially underestimating multi-decadal climate variability (see Kravtsov, 2017; Kravtsov et al., 2018). This discrepancy could arise from several factors, including coarse spatial resolution, an unrealistic representation of overturning circulation and ocean eddies, or weak ocean−atmosphere and climate feedbacks in climate models (Roberts et al., 2020; Scaife & Smith, 2018). Notably, we find significant correlations between the observed NAO and subpolar ocean temperature anomalies at negative lag years (black curve, Figure 4a). However, climate models lack any such correlations. These results indicate that the sensitivity of the atmosphere, particularly the NAO-type response, to ocean temperatures may be too weak in climate models.

Conflict of Interest

The authors declare no conflicts of interest relevant to this study.

Data Availability Statement

Climate model outputs used in this work can be accessed via CMIP6 archive https://esgf-index1.ceda.ac.uk/projects/cmip6-ceda/ and are also hosted on CEDA archive (www.ceda.ac.uk/). Observational data sets can be

downloaded from the UK Met Office website: EN4 data from https://www.metoffice.gov.uk/hadobs/en4/, HadISST data from https://www.metoffice.gov.uk/hadobs/hadisst/, and HadSLP2 data from https://www.metoffice.gov.uk/hadobs/hadslp2/. Post-processed data and python scripts used for analysis are available at Khatri (2024) and https://github.com/hmkhatri/Ocean-Memory-Atlantic-GRL-2024.

Acknowledgments
We thank the two anonymous reviewers for their reviews and feedback. The authors acknowledge the support from the Natural Environment Research Council Grant NE/T013494/1. JASMIN (http://jasmin.ac.uk/) and CEDA (www.ceda.ac.uk/) facilities were used for the computations. DMS was supported by the Met Office Hadley Centre Climate Programme funded by BEIS and Defra.

References

Allan, R., & Ansell, T. (2006). A new globally complete monthly historical gridded mean sea level pressure dataset (HadSLP2): 1850–2004. *Journal of Climate*, *19*(22), 5816–5842. https://doi.org/10.1175/JCLI3937.1

Barrier, N., Cassou, C., Deshayes, J., & Treguier, A.-M. (2014). Response of North Atlantic Ocean circulation to atmospheric weather regimes. *Journal of Physical Oceanography*, *44*(1), 179–201. https://doi.org/10.1175/JPO-D-12-0217.1

Bjerknes, J. (1964). Atlantic air-sea interaction. *Advances in Geophysics*, *10*, 1–82. https://doi.org/10.1016/s0065-2687(08)60005-9

Boucher, O., Servonnat, J., Albright, A. L., Aumont, O., Balkanski, Y., Bastrikov, V., et al. (2020). Presentation and evaluation of the IPSL-CM6A-LR climate model. *Journal of Advances in Modeling Earth Systems*, *12*(7), e2019MS002010. https://doi.org/10.1029/2019MS002010

Cane, M. A., Clement, A. C., Murphy, L. N., & Bellomo, K. (2017). Low-pass filtering, heat flux, and Atlantic multidecadal variability. *Journal of Climate*, *30*(18), 7529–7553. https://doi.org/10.1175/JCLI-D-16-0810.1

Clement, A., Bellomo, K., Murphy, L. N., Cane, M. A., Mauritsen, T., Rädel, G., & Stevens, B. (2015). The Atlantic multidecadal oscillation without a role for ocean circulation. *Science*, *350*(6258), 320–324. https://doi.org/10.1126/science.aab3980

Cornish, S. B., Kostov, Y., Johnson, H. L., & Lique, C. (2020). Response of arctic freshwater to the arctic oscillation in coupled climate models. *Journal of Climate*, *33*(7), 2533–2555. https://doi.org/10.1175/jcli-d-19-0685.1

Danabasoglu, G., Lamarque, J.-F., Bacmeister, J., Bailey, D., DuVivier, A., Edwards, J., et al. (2020). The community Earth system model version 2 (CESM2). *Journal of Advances in Modeling Earth Systems*, *12*(2), e2019MS001916. https://doi.org/10.1029/2019MS001916

Delworth, T. L., & Mann, M. E. (2000). Observed and simulated multidecadal variability in the northern hemisphere. *Climate Dynamics*, *16*(9), 661–676. https://doi.org/10.1007/s003820000075

Delworth, T. L., Zeng, F., Zhang, L., Zhang, R., Vecchi, G. A., & Yang, X. (2017). The central role of ocean dynamics in connecting the North Atlantic oscillation to the extratropical component of the Atlantic multidecadal oscillation. *Journal of Climate*, *30*(10), 3789–3805. https://doi.org/10.1175/JCLI-D-16-0358.1

Deser, C., Alexander, M. A., Xie, S.-P., & Phillips, A. S. (2010). Sea surface temperature variability: Patterns and mechanisms. *Annual Review of Marine Science*, *2*(1), 115–143. https://doi.org/10.1146/annurev-marine-120408-151453

Eden, C., & Jung, T. (2001). North atlantic interdecadal variability: Oceanic response to the North Atlantic oscillation (1865–1997). *Journal of Climate*, *14*(5), 676–691. https://doi.org/10.1175/1520-0442(2001)014⟨0676:NAIVOR⟩2.0.CO;2

Eden, C., & Willebrand, J. (2001). Mechanism of interannual to decadal variability of the North Atlantic circulation. *Journal of Climate*, *14*(10), 2266–2280. https://doi.org/10.1175/1520-0442(2001)014⟨2266:MOITDV⟩2.0.CO;2

Frankignoul, C., & Hasselmann, K. (1977). Stochastic climate models, Part II: Application to sea-surface temperature anomalies and thermocline variability. *Tellus*, *29*(4), 289–305. https://doi.org/10.3402/tellusa.v29i4.11362

Fraser, N. J., & Cunningham, S. A. (2021). 120 years of AMOC variability reconstructed from observations using the Bernoulli inverse. *Geophysical Research Letters*, *48*(18), e2021GL093893. https://doi.org/10.1029/2021GL093893

Good, S. A., Martin, M. J., & Rayner, N. A. (2013). EN4: Quality controlled ocean temperature and salinity profiles and monthly objective analyses with uncertainty estimates. *Journal of Geophysical Research: Oceans*, *118*(12), 6704–6716. https://doi.org/10.1002/2013JC009067

Gozdz, O., Buckley, M. W., & DelSole, T. (2024). The impact of interactive ocean dynamics on Atlantic Sea surface temperature variability. *Journal of Climate*, *37*(10), 2937–2964. https://doi.org/10.1175/JCLI-D-23-0609.1

Gu, P., Liu, Z., & Delworth, T. L. (2024). Strong oceanic forcing on decadal surface temperature variability over global ocean. *Geophysical Research Letters*, *51*(8), e2023GL107401. https://doi.org/10.1029/2023GL107401

Gulev, S. K., Latif, M., Keenlyside, N., Park, W., & Koltermann, K. P. (2013). North Atlantic Ocean control on surface heat flux on multidecadal timescales. *Nature*, *499*(7459), 464–467. https://doi.org/10.1038/nature12268

Hansen, D. V., & Bezdek, H. F. (1996). On the nature of decadal anomalies in North Atlantic sea surface temperature. *Journal of Geophysical Research*, *101*(C4), 8749–8758. https://doi.org/10.1029/95JC03841

Hasselmann, K. (1976). Stochastic climate models, Part I: Theory. *Tellus*, *28*(6), 473–485. https://doi.org/10.3402/tellusa.v28i6.11316

Hasselmann, K., Sausen, R., Maier-Reimer, E., & Voss, R. (1993). On the cold start problem in transient simulations with coupled atmosphere-ocean models. *Climate Dynamics*, *9*(2), 53–61. https://doi.org/10.1007/BF00210008

Held, I., Guo, H., Adcroft, A., Dunne, J., Horowitz, L., Krasting, J., et al. (2019). Structure and performance of GFDL's CM4. 0 Climate model. *Journal of Advances in Modeling Earth Systems*, *11*(11), 3691–3727. https://doi.org/10.1029/2019MS001829

Hurrell, J. W. (1995). Decadal trends in the North Atlantic oscillation: Regional temperatures and precipitation. *Science*, *269*(5224), 676–679. https://doi.org/10.1126/science.269.5224.676

Hurrell, J. W., & Deser, C. (2010). North Atlantic climate variability: The role of the North Atlantic oscillation. *Journal of Marine Systems*, *79*(3–4), 231–244. https://doi.org/10.1016/j.jmarsys.2009.11.002

Jackson, L. C., Biastoch, A., Buckley, M. W., Desbruyères, D. G., Frajka-Williams, E., Moat, B., & Robson, J. (2022). The evolution of the North Atlantic meridional overturning circulation since 1980. *Nature Reviews Earth & Environment*, *3*(4), 241–254. https://doi.org/10.1038/s43017-022-00263-2

Johnson, H. L., Cornish, S. B., Kostov, Y., Beer, E., & Lique, C. (2018). Arctic Ocean freshwater content and its decadal memory of sea-level pressure. *Geophysical Research Letters*, *45*(10), 4991–5001. https://doi.org/10.1029/2017GL076870

Josey, S. A., & Sinha, B. (2022). Subpolar Atlantic Ocean mixed layer heat content variability is increasingly driven by an active ocean. *Communications Earth & Environment*, *3*(1), 1–8. https://doi.org/10.1038/s43247-022-00433-6

Khatri, H. (2024). Post-processed dataset: An ocean memory approach for analysing decadal variability in the North Atlantic Ocean. *Zenodo*. https://doi.org/10.5281/zenodo.13306350

Khatri, H., Williams, R. G., Woollings, T., & Smith, D. M. (2022). Fast and slow subpolar ocean responses to the North Atlantic Oscillation: Thermal and dynamical changes. *Geophysical Research Letters*, *49*(24), e2022GL101480. https://doi.org/10.1029/2022GL101480

Khurshut, L. T. (1994). Interdecadal variations in North Atlantic Sea surface temperature and associated atmospheric conditions. *Journal of Climate*, *7*(1), 141–155. https://doi.org/10.1175/1520-0442(1994)007⟨0141:IVINAST⟩2.0.CO;2

Kim, W. M., Ruprich-Robert, Y., Zhao, A., Yeager, S., & Robson, J. (2024). North Atlantic response to observed North Atlantic Oscillation surface heat flux in three climate models. *Journal of Climate*, *37*(5), 1777–1796. https://doi.org/10.1175/JCLI-D-23-0301.1

Knight, J. R., Folland, C. K., & Scaife, A. A. (2006). Climate impacts of the Atlantic multidecadal oscillation. *Geophysical Research Letters*, *33*(17). https://doi.org/10.1029/2006GL026242

Kostov, Y., Marshall, J., Hausmann, U., Armour, K. C., Ferreira, D., & Holland, M. M. (2017). Fast and slow responses of southern ocean sea surface temperature to Sam in coupled climate models. *Climate Dynamics*, *48*(5–6), 1595–1609. https://doi.org/10.1007/s00382-016-3162-z

Kravtsov, S. (2017). Pronounced differences between observed and CMIP5-simulated multidecadal climate variability in the twentieth century. *Geophysical Research Letters*, *44*(11), 5749–5757. https://doi.org/10.1002/2017GL074016

Kravtsov, S., Grimm, C., & Gu, S. (2018). Global-scale multidecadal variability missing in state-of-the-art climate models. *npj Climate and Atmospheric Science*, *1*(1), 34. https://doi.org/10.1038/s41612-018-0044-6

Leith, C. E. (1975). Climate response and fluctuation dissipation. *Journal of the Atmospheric Sciences*, *32*(10), 2022–2026. https://doi.org/10.1175/1520-0469(1975)032⟨2022:CRAFD⟩2.0.CO;2

Liu, Z., Gu, P., & Delworth, T. L. (2023). Strong red noise ocean forcing on Atlantic multidecadal variability assessed from surface heat flux: Theory and application. *Journal of Climate*, *36*(1), 55–80. https://doi.org/10.1175/JCLI-D-22-0063.1

Lozier, M. S., Leadbetter, S., Williams, R. G., Roussenov, V., Reed, M. S., & Moore, N. J. (2008). The spatial pattern and mechanisms of heat-content change in the North Atlantic. *Science*, *319*(5864), 800–803. https://doi.org/10.1126/science.1146436

Marshall, J., Johnson, H., & Goodman, J. (2001a). A study of the interaction of the North Atlantic Oscillation with ocean circulation. *Journal of Climate*, *14*(7), 1399–1421. https://doi.org/10.1175/1520-0442(2001)014⟨1399:ASOTIO⟩2.0.CO;2

Marshall, J., Kushnir, Y., Battisti, D., Chang, P., Czaja, A., Dickson, R., et al. (2001b). North Atlantic climate variability: Phenomena, impacts and mechanisms. *International Journal of Climatology: A Journal of the Royal Meteorological Society*, *21*(15), 1863–1898. https://doi.org/10.1002/joc.693

McCarthy, G. D., Haigh, I. D., Hirschi, J. J.-M., Grist, J. P., & Smeed, D. A. (2015). Ocean impact on decadal Atlantic climate variability revealed by sea-level observations. *Nature*, *521*(7553), 508–510. https://doi.org/10.1038/nature14491

Monerie, P.-A., Robson, J., Dong, B., Hodson, D. L., & Klingaman, N. P. (2019). Effect of the Atlantic multidecadal variability on the global monsoon. *Geophysical Research Letters*, *46*(3), 1765–1775. https://doi.org/10.1029/2018gl080903

Namias, J., & Born, R. M. (1970). Temporal coherence in North Pacific sea-surface temperature patterns. *Journal of Geophysical Research*, *75*(30), 5952–5955. https://doi.org/10.1029/jc075i030p05952

O'Reilly, C. H., Huber, M., Woollings, T., & Zanna, L. (2016). The signature of low-frequency oceanic forcing in the Atlantic multidecadal oscillation. *Geophysical Research Letters*, *43*(6), 2810–2818. https://doi.org/10.1002/2016GL067925

O'Reilly, C. H., & Zanna, L. (2018). The signature of oceanic processes in decadal extratropical SST anomalies. *Geophysical Research Letters*, *45*(15), 7719–7730. https://doi.org/10.1029/2018GL079077

Patrizio, C. R., Athanasiadis, P. J., Frankignoul, C., Iovino, D., Masina, S., Famooss Paolini, L., & Gualdi, S. (2023). Improved extratropical North Atlantic atmosphere–ocean variability with increasing ocean model resolution. *Journal of Climate*, *36*(24), 8403–8424. https://doi.org/10.1175/JCLI-D-23-0230.1

Rayner, N., Parker, D. E., Horton, E., Folland, C. K., Alexander, L. V., Rowell, D., et al. (2003). Global analyses of sea surface temperature, sea ice, and night marine air temperature since the late nineteenth century. *Journal of Geophysical Research*, *108*(D14). https://doi.org/10.1029/2002JD002670

Roberts, M. J., Jackson, L. C., Roberts, C. D., Meccia, V., Docquier, D., Koenigk, T., et al. (2020). Sensitivity of the Atlantic meridional overturning circulation to model resolution in CMIP6 HighResMIP simulations and implications for future changes. *Journal of Advances in Modeling Earth Systems*, *12*(8), e2019MS002014. https://doi.org/10.1029/2019MS002014

Robson, J., Ortega, P., & Sutton, R. (2016). A reversal of climatic trends in the North Atlantic since 2005. *Nature Geoscience*, *9*(7), 513–517. https://doi.org/10.1038/ngeo2727

Robson, J., Sutton, R., Lohmann, K., Smith, D., & Palmer, M. D. (2012). Causes of the rapid warming of the North Atlantic Ocean in the mid-1990s. *Journal of Climate*, *25*(12), 4116–4134. https://doi.org/10.1175/JCLI-D-11-00443.1

Roussenov, V. M., Williams, R. G., Lozier, M. S., Holliday, N. P., & Smith, D. M. (2022). Historical reconstruction of subpolar North Atlantic overturning and its relationship to density. *Journal of Geophysical Research: Oceans*, *127*(6), e2021JC017732. https://doi.org/10.1029/2021JC017732

Saravanan, R., & McWilliams, J. C. (1998). Advective ocean–atmosphere interaction: An analytical stochastic model with implications for decadal variability. *Journal of Climate*, *11*(2), 165–188. https://doi.org/10.1175/1520-0442(1998)011⟨0165:AOAIAA⟩2.0.CO;2

Scaife, A. A., & Smith, D. (2018). A signal-to-noise paradox in climate science. *npj Climate and Atmospheric Science*, *1*(1), 28. https://doi.org/10.1038/s41612-018-0038-4

Shi, H., Jin, F.-F., Wills, R. C., Jacox, M. G., Amaya, D. J., Black, B. A., et al. (2022). Global decline in ocean memory over the 21st century. *Science Advances*, *8*(18), eabm3468. https://doi.org/10.1126/sciadv.abm3468

Visbeck, M., Cullen, H., Krahmann, G., & Naik, N. (1998). An ocean model's response to North Atlantic Oscillation-like wind forcing. *Geophysical Research Letters*, *25*(24), 4521–4524. https://doi.org/10.1029/1998GL900162

Williams, K., Copsey, D., Blockley, E., Bodas-Salcedo, A., Calvert, D., Comer, R., et al. (2018). The Met Office global coupled model 3.0 and 3.1 (GC3. 0 and GC3. 1) configurations. *Journal of Advances in Modeling Earth Systems*, *10*(2), 357–380. https://doi.org/10.1002/2017MS001115

Williams, R. G., Roussenov, V., Lozier, M. S., & Smith, D. (2015). Mechanisms of heat content and thermocline change in the subtropical and subpolar North Atlantic. *Journal of Climate*, *28*(24), 9803–9815. https://doi.org/10.1175/JCLI-D-15-0097.1

Williams, R. G., Roussenov, V., Smith, D., & Lozier, M. S. (2014). Decadal evolution of ocean thermal anomalies in the North Atlantic: The effects of Ekman, overturning, and horizontal transport. *Journal of Climate*, *27*(2), 698–719. https://doi.org/10.1175/JCLI-D-12-00234.1

Woollings, T., Franzke, C., Hodson, D., Dong, B., Barnes, E. A., Raible, C., & Pinto, J. (2015). Contrasting interannual and multidecadal NAO variability. *Climate Dynamics*, *45*(1–2), 539–556. https://doi.org/10.1007/s00382-014-2237-y

Woollings, T., Hannachi, A., & Hoskins, B. (2010). Variability of the North Atlantic eddy-driven jet stream. *Quarterly Journal of the Royal Meteorological Society*, *136*(649), 856–868. https://doi.org/10.1002/qj.625

Zhang, R. (2017). On the persistence and coherence of subpolar sea surface temperature and salinity anomalies associated with the Atlantic multidecadal variability. *Geophysical Research Letters*, *44*(15), 7865–7875. https://doi.org/10.1002/2017GL074342

Zhang, R., & Delworth, T. L. (2006). Impact of Atlantic multidecadal oscillations on India/Sahel rainfall and Atlantic hurricanes. *Geophysical Research Letters*, *33*(17). https://doi.org/10.1029/2006GL026267

Zhang, R., Sutton, R., Danabasoglu, G., Kwon, Y.-O., Marsh, R., Yeager, S. G., et al. (2019). A review of the role of the Atlantic meridional overturning circulation in Atlantic multidecadal variability and associated climate impacts. *Reviews of Geophysics*, *57*(2), 316–375. https://doi.org/10.1029/2019RG000644